CHEMISTRY OF MATERIALS

ARTICLE

pubs.acs.org/cm

# Combined Covalent and Noncovalent Functionalization of Nanomagnetic Carbon Surfaces with Dendrimers and BODIPY Fluorescent Dye

Quirin M. Kainz,[†] Alexander Schätz,[‡] Alexander Zöpfl,[†] Wendelin J. Stark,[‡] and Oliver Reiser*[,†]

[†]Institut für Organische Chemie, Universität Regensburg, Universitätsstr. 31, 93053 Regensburg, Germany

[‡]Institut für Chemie- und Bioingenieurwissenschaften, Department Chemie und Angewandte Biowissenschaften, ETH Zürich, Wolfgang-Pauli-Strasse 10, 8093 Zürich, Switzerland

Supporting Information

**ABSTRACT:** A general method for the synthesis of multifunctional carbon nanomaterials following an unprecedented combined covalent and noncovalent immobilization strategy is reported. Highly magnetic (158 emu/g) carbon-coated cobalt nanoparticles (Co/C) served as scaffold for noncovalent functionalization of pyrene-tagged boradiazaindacene (BODIPY) fluorescent dye through $\pi-\pi$ stacking interactions. Next to the reversibly immobilized pyrene-tagged dye, fully covalent functionalization of the magnetic core/shell nanoparticles was accomplished by grafting dendrimers via diazonium/"click"-chemistry. Alternatively, the nanoparticle surface could be covalently functionalized with BODIPY dye following same procedure. The Co/C nanomagnets labeled with fluorescent dye were further examined by confocal laser scanning microscopy (CLSM). Because of the strong fluorescence and magnetic remanence, this material might be interesting for imaging applications and as a nanosized carrier for reversibly attached drugs.

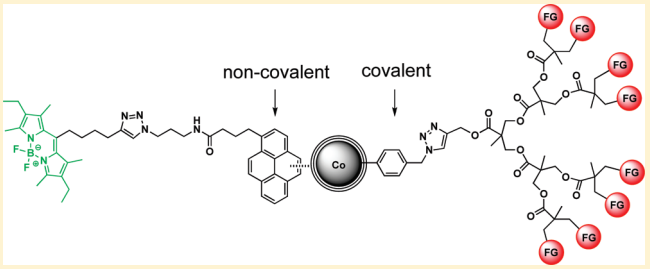


**KEYWORDS:** covalent and noncovalent multifunctionalization, magnetic nanoparticles, fluorescent nanomagnets, BODIPY, dendrimer, imaging

## INTRODUCTION

The greatest goal in modern nanoscience might be to render matter molecule-like not only by reducing its dimensions but especially by installing multiple functionalities that break ground for complex chemistry as well as biochemistry. The surfaces of graphene-based entities such as fullerenes,[1] carbon nanotubes (CNTs),[2] or carbon-coated metal nanoparticles[3] are arguably most attractive for functionalized nanoscale materials because they enable the formation of covalent C−C bonds. Hence, surface chemistry on such nanomaterials is rich, comprising oxidative strategies, various cycloaddition reactions, and diazonium chemistry among others.[1−3] Multifunctional entities and assemblies could be achieved through mixtures of compounds[4] by installing complex multifunctional molecules[5] or by means of two consecutive functionalization strategies.[6] However, all these strategies rely on the combination of covalent binding modes, thus taking exclusively the chemical character of the nanomaterial into account.

Recently, it was reported that nanosized carbon scaffolds can be noncovalently modified with aromatic compounds (e.g., pyrene) via $\pi-\pi$ stacking interactions.[7] The latter strategy is described as a physical rather than chemical interaction with the material, which therefore allows the release of the immobilized molecules under elevated temperatures or by switching the solvent.[8] It is surprising that the combination of such a potentially reversible patterning and an irreversible chemical bonding for multifunctional nanomaterials has yet to be reported because it reflects perfectly the interplay of macroscopic properties and molecule-character in the threshold of both. Hence, such a combined covalent and noncovalent approach could significantly broaden the scope of nanomaterials, e.g., for the controlled and monitored release of drugs.

Even more versatile materials might arise if highly magnetic core materials coated by graphene-layers are used. Such systems exist as "metal-filled" nanotubes[9] or more stable core/shell nanoparticles.[3,10] Promising medical applications for magnetic nanomaterials are, among others, magnetic drug targeting,[11] magnetic resonance imaging (MRI),[12] and magnetic fluid hyperthermia (MFH).[13] However, all these applications would benefit from nanomaterials with higher magnetization than the commonly used superparamagnetic iron oxide nanoparticles (SPION, $M_{s,\ bulk} \leq 92$ emu/g).[14] The magnetization of these SPIONs is typically further diminished upon surface modification.

**Received:** March 9, 2011
**Revised:** June 17, 2011
**Published:** July 20, 2011

Recently, Stark et al.[3a] reported a new continuous process for the production of ferromagnetic Co/C nanoparticles on multigram scale (30 g/h) via reducing flame spray pyrolysis. The relatively thin (1−3 nm), yet effective, coating of the metal core with graphene-like layers leads to an impressive thermal as well as chemical stability of the nanoparticles.[15] Furthermore, the carbon shell has no detrimental effect on the magnetization (158 emu/g). Herein, we report the first combination of covalent and noncovalent functionalization of these carbon encapsulated, highly magnetic nanoparticles. As the covalent part, 2,2-bis(hydroxymethyl) propionic acid (bis-MPA)-based dendrimers were chosen because they render one functional group at the surface of the particles into an array of moieties.[16] This feature is highly desired for the attachment of sufficient quantities of bioactive molecules, e.g., folate, sugars, peptides, or antibodies, to target specific receptors on cell surfaces.[17] Additionally, the attachment of anticancer drugs at the dendrimer periphery through pH-sensitive linkers has been realized.[18] For the noncovalent coating, a fluorescent probe connected to a pyrene molecule was chosen for possible applications of the labeled magnetic nanoparticles in bioimaging, e.g., as dual imaging probes,[19] in which fluorescence microscopy is combined with MRI.

It has been reported that fluorescent dyes such as fluorescein and rhodamine,[20] as well as pyrenes[21] are effectively quenched by graphene-like carbon surfaces, e.g., carbon nanotubes. While this quenching effect can be useful in the field of biosensing,[22] it is highly undesired when it comes to bioimaging. Therefore, within this study a boradiazaindacene (BODIPY) dye [23] was chosen, which features a considerably smaller $\pi$-system compared to fluorescein or pyrene dyes. Consequently, interactions with the graphene-like surface should be diminished and thus reduce the quenching effect. Further attractive properties of the BODIPY dyes are high fluorescence quantum yield and molar absorptivity, good photochemical stability, and the fact that their fluorescence properties can easily be altered by varying the substitution pattern on the core and the flanking pyrroles to match the emission wavelengths of lasers applied in bioimaging.[24]

## EXPERIMENTAL SECTION

**Materials and Methods.** The carbon-coated cobalt nanomagnets (Co/C, 20.5 $m^2$/g, mean particle size ≈25 nm)[3d] were purchased from Turbobeads Llc, Switzerland. Prior to use, they were washed in a concentrated HCl (Merck, puriss)/deionized water (Millipore) mixture (1:1) 5 times for 24 h. Acid residuals were removed by washing with Millipore water (5x) and the particles were dried at 50 °C in a vacuum oven.[25] 4,4-Difluoro-8-(hept-6-yne)-1,3,5,7-tetramethyl-2,6-diethyl-4-bora-3a,4a-diaza-s-indacene,[24] *N*-(3-azidopropyl)-4-(pyren-1-yl) butanamide,[26] azide functionalized Co/C nanoparticles (loading: 0.14 mmol/g),[3c] Acet-[G3]-$(OH)_8$[30], and Acet-[G3]-$(NH_3^+TFA^-)_8$[31] were prepared according to literature procedures. All other commercially available compounds were used as received. $^1$H NMR (600 MHz) spectra were recorded in $CDCl_3$ with $CHCl_3$ (7.26 ppm) as a standard. $^{13}$C NMR (75.5 MHz) spectra were recorded in $CDCl_3$ with $CHCl_3$ (77 ppm) as a standard. Analytical thin layer chromatography was performed on TLC aluminum sheets coated with silica gel 60 F254. Visualization was accomplished with UV light and vaniline solution followed by heating. Liquid chromatography was performed using silica gel 60 (70−230 mesh ASTM). UV/vis spectra were measured using a Varian Cary 50 Bio spectrometer, and fluorescence data was recorded on a JASCO FP-6300 spectrometer. Magnetic nanobeads were dispersed using an ultrasound bath and recovered with the aid of a neodymium-based magnet (side length 12 mm). They were characterized by ATR-IR spectroscopy equipped with a (Specac *Golden Gate* Diamond Single Reflection ATR-System), elemental microanalysis (LECO CHN-900), transmission electron microscopy (Zeiss, LEO912AB, 100 kV), and confocal laser scanning microscopy on a laser scanning microscope (Zeiss, LSM510) equipped with an argon laser, emitting at 514 nm.

**Nomenclature.** The nomenclature for dendritic structures described in in this work is as follows: FG-[G*X*]-(R)*n* for dendrimers, where *X* indicates the generation of the dendritic framework. FG describes the functional group at the focal point where Acet represents acetylene and R describes the external functional group, which can be OH for hydroxyl or $NH_3^+$ $TFA^-$ for unprotected amine.

**Synthesis of Pyrene-Tagged BODIPY (3).** A total of 48 mg (124 $\mu$mol) of BODIPY-alkyne **2** and 52 mg (160 $\mu$mol) of pyrene-azide **1** were dissolved in 2 mL of degassed $CH_2Cl_2$. $Et_3N$ (20 $\mu$L, 145 $\mu$mol) and CuI (1.4 mg, 7 $\mu$mol) were successively added, and the reaction mixture was stirred at ambient temperature for 24 h. Then, the solvent was evaporated under reduced pressure, and the crude product was purified by column chromatography eluting with $CH_2Cl_2$ and gradually increasing the polarity by addition of MeOH to the final composition of 20%. After evaporation of the solvents, 93 mg (123 $\mu$mol, 99%) of the red solid **3** were isolated. Detailed characterization ($^1$H NMR, $^{13}$C NMR, IR, HR-Mass, UV/vis and fluorescence spectra) can be found in the Supporting Information.

**Pyrene-BODIPY Functionalized Carbon-Coated Cobalt Nanoparticles (5).** Carbon-coated cobalt nanoparticles **4** (30 mg) were dispersed in 5 mL of $H_2O$ by sonication in an ultrasonic bath for 10 min. Pyrene-labeled BODIPY (4.5 mg, 6 $\mu$mol) **3** was added, and the sonication continued for 1 h. Then, the particles were recovered by the aid of a neodymium magnet. The particles were washed by sonication in water (5 mL) for 15 min, followed by magnetic decantation. This washing procedure was repeated 15 times, yielding 31 mg of functionalized particles **5**. IR ($\nu$/cm$^{-1}$): 2936, 2874, 1657, 1547, 1481, 1331, 1068, 982, 845. Elemental microanalysis (%): C, 9.72; H, 0.47; N, 0.33. $\lambda_{em}$: 533 nm.

**BODIPY Dye Covalently Immobilized on Carbon-Coated Cobalt Nanoparticles (7).** A total of 100 mg of azide functionalized Co/C particles **6** were predispersed in 2 mL of degassed $CH_2Cl_2$ for 10 min, followed by addition of 18.3 mg (50 $\mu$mol) acetylene functionalized BODIPY **2**, 1 mg (5 $\mu$mol) CuI, and 7 $\mu$L (50 $\mu$mol) triethylamine. The mixture was then dispersed for 1 h by sonication using an ultrasonic bath and afterward placed on a laboratory shaker (Köttermann type 4018, level 7) for 48 h. The magnetic nanoparticles were recovered with a magnet and thoroughly washed with toluene (15 × 5 mL) by sonication for 15 min, followed by magnetic decantation after each washing step. After drying under high vacuum, 98 mg of the particles **7** were retained. IR ($\nu$/cm$^{-1}$): 2963, 2929, 2870, 1698, 1542, 1476, 1405, 1328, 1191, 1061, 1044, 977, 804, 721, 647, 598, 534. Elemental microanalysis (%): C, 8.89; H, 0.22; N, 0.64. $\lambda_{em}$: 524 nm.

**[G3]-$(OH)_8$ Covalently Functionalized Carbon-Coated Cobalt Nanoparticles (10).** Azide functionalized carbon-coated cobalt nanoparticles **6** (100 mg) were dispersed in 3 mL of a degassed THF/$H_2O$ 3:1 mixture. Then, 44 mg (50 $\mu$mol) of Acet-[G3]-$(OH)_8$ **8**, $CuSO_4 \cdot 5H_2O$ (1.2 mg, 5 $\mu$mol), and sodium ascorbate (3 mg, 15 $\mu$mol) were added successively. The mixture was sonicated for 1 h and thereafter put on the laboratory shaker for 24 h. After intensive washing with acetone (5 × 5 mL) and water (5 × 5 mL), 101 mg of the nanoparticles were recovered with the aid of a magnet and dried under high vacuum. IR ($\nu$/cm$^{-1}$): 2959, 2901, 1738, 1474, 1242, 1134, 1038. Elemental microanalysis (%): C, 8.17; H, 0.34; N, 0.35.

**Carbon-Coated Cobalt Nanoparticles Covalently Functionalized with [G3]-$(NH_3^+TFA^-)_8$ (11).** After dispersing azide functionalized cobalt nanoparticles **6** (100 mg) in 3 mL of a degassed THF/$H_2O$ 3:1 mixture, 118 mg (50 $\mu$mol) of Acet-[G3]-$(NH_3^+TFA^-)_8$ **9**

**Scheme 1. Synthesis of Pyrene-Tagged BODIPY Fluorescent Dye**

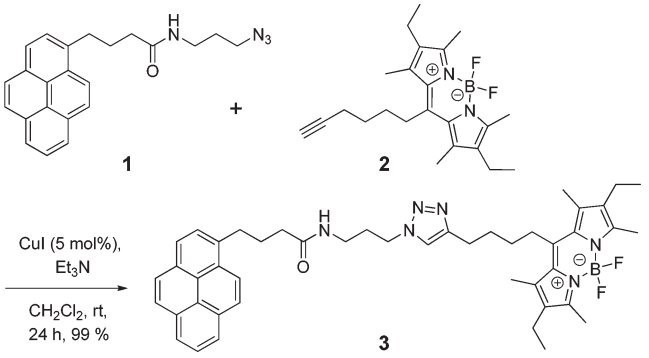


was added. Then $CuSO_4 \cdot 5H_2O$ (1.2 mg, 5 $\mu$mol) and sodium ascorbate (3 mg, 15 $\mu$mol) were added successively. The mixture was first sonicated for 1 h and then put on the laboratory shaker for 24 h. The functionalized particles were separated with the aid of a magnet and washed with acetone (5 × 5 mL) and $H_2O$ (5 × 5 mL), followed by magnetic decantation after each washing step. Recovery from the reaction mixture and drying under vacuum yielded 101 mg of nanoparticles **11**. IR ($\nu$/cm$^{-1}$): 2929, 2849, 1735, 1659, 1466, 1126, 806, 691. Elemental microanalysis (%): C, 8.45; H, 0.35; N, 0.6.

**[G3]-(OH)$_8$ Covalently and Pyrene-BODIPY Noncovalently Functionalized Carbon-Coated Cobalt Nanoparticles (12).** A total of 20 mg of dendrimer functionalized nanoparticles **10** were dispersed in 3 mL of $H_2O$ before pyrene-BODIPY **3** (4.2 mg, 5.6 $\mu$mol) was added. The slurry was sonicated for 1 h and then washed with water (10 × 5 mL), following the common procedure. Magnetic decantation and drying led to 20 mg of nanoparticles **12**. IR ($\nu$/cm$^{-1}$): 2967, 2940, 2864, 1734, 1674, 1545, 1479, 1329, 1198, 1140, 1049, 982, 847. Elemental microanalysis (%): C, 17.68; H, 1.28; N, 1.94. $\lambda_{em}$: 534 nm.

**[G3]-(NH$_3^+$TFA$^-$)$_8$ Covalently and Pyrene-BODIPY Noncovalently Functionalized Carbon-Coated Cobalt Nanoparticles (13).** After dispersing 50 mg of [G3]-(NH$_3^+$TFA$^-$)$_8$ covalently functionalized nanoparticles **11** in 3 mL of $H_2O$, 10.5 mg of pyrene-tagged BODIPY **3** (14 $\mu$mol) was added, followed by further sonication for 1 h. The particles were recovered by the aid of a magnet and thoroughly washed with water (10 mL × 5 mL). After drying, 48 mg of functionalized nanoparticles were yielded. IR ($\nu$/cm$^{-1}$): 2938, 2880, 2112, 1740, 1667, 1545, 1479, 1331, 1198, 1065, 984, 847. Elemental microanalysis (%): C, 16.10; H, 1.2; N, 1.77. $\lambda_{em}$: 534 nm.

**Control Experiment To Examine Interactions between Pyrene-BODIPY and Acet-[G3]-(OH)$_8$ Dendrimers.** To a solution of 3.8 mg (4.3 $\mu$mol) Acet-[G3]-(OH)$_8$ **8** in 2 mL $H_2O$ was added 3.3 mg (4.3 $\mu$mol) of pyrene-BODIPY **3**. The mixture was then sonicated for 1 h using an ultrasonic bath following the procedure for the noncovalent attachment of dye **3** onto dendrimer-modified nanoparticles. The slightly reddish solution was filtrated over a frit to remove undissolved dye. A total of 500 $\mu$L of the filtrate were freeze-dried, and the residue was collected in 2 mL of toluene. A control experiment was performed without the addition of dendrimers **8**. The fluorescence intensities of the toluene solutions were measured at an excitation wavelength of 515 nm, and the concentration of dye **3** was determined by comparison with reference solutions of **3** in toluene.

**Release Study of Pyrene-BODIPY from Multifunctionalized Nanoparticles 13.** A total of 1.0 mg of [G3]-(NH$_3^+$TFA$^-$)$_8$ covalently and pyrene-BODIPY noncovalently functionalized carbon-coated cobalt nanoparticles **13** were stirred in toluene for 2 h by exploiting the magnetic properties of the nanobeads. The nanoparticles were collected by the aid of an external magnet, and the solution was

**Scheme 2. Noncovalent (top) and Covalent (bottom) Functionalization of Magnetic Co/C Nanoparticles**

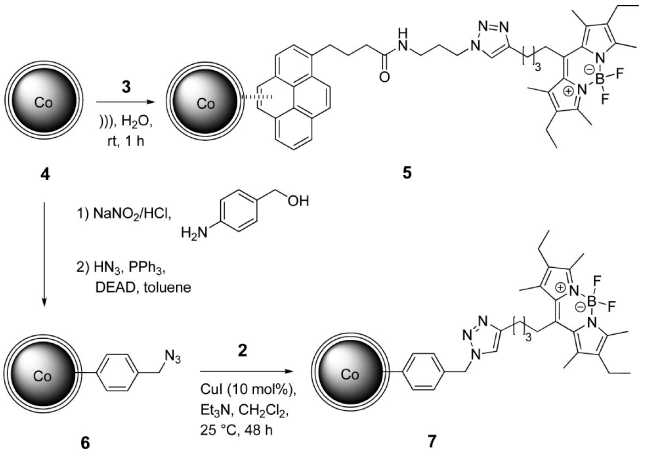


decanted. This process was repeated twice, and the fluorescences of the washing solutions were measured at an excitation wavelength of 515 nm. The concentration of free dye was determined by comparing the fluorescence intensities with reference solutions of Pyrene-BODIPY **3** in toluene.

## RESULTS AND DISCUSSION

The pyrene-tagged BODIPY dye **3** was readily synthesized in excellent yields by a copper-catalyzed azide/alkyne cycloaddition (CuAAC),[27] a so-called "click"-reaction, between azide functionalized pyrene **1** and alkyne modified BODIPY **2** (Scheme 1). UV/vis measurements revealed an absorption maximum at 518 nm, and fluorescence spectroscopy showed an emission maximum at 534 nm. Because of the low solubility of **3** in water, the spectra were recorded in dichloromethane,[28] and the values obtained correspond with those of unmodified dye **2** (519 nm/529 nm).[24] Noncovalent immobilization of **3** onto the surface of magnetic Co/C nanoparticles **4** was achieved by sonication in water for 1 h (Scheme 2). The nanoparticles were then recovered with the aid of a neodymium-based magnet and washed extensively with water followed by magnetic decantation after each washing step to remove unbound dye. The attachment of the dye was proved by ATR-IR spectroscopy,[28] and the loading of the nanoparticles with **3** was determined by elemental microanalysis to be 0.05 mmol/g.

Alternatively, the covalent attachment of a BODIPY dye to the magnetic nanoparticles was also examined (Scheme 2). Azide-functionalized particles **6** were prepared in two steps from pristine nanobeads **4** through grafting of diazonium ions and subsequent Mitsunobu reaction, following literature procedures.[3c] Fluorescent dye **2** was then "clicked" onto the azide functionalized Co/C nanoparticles **6** using the copper-catalyzed (CuI/Et$_3$N)[27d] azide−alkyne cycloaddition (CuACC) reaction. To remove unbound dye, the particles were copiously washed with toluene. A comparison of up to 30 consecutive washing solutions revealed that the fluorescence intensity dropped rapidly in about 10 washing steps and then stayed constant for the next 20 steps at a very low level.[28] This observation could be explained with the presence of trace amounts of nonmagnetic carbon-based nanomaterial, which is nevertheless functionalized with BODIPY dye. The completion of the functionalization step was monitored by ATR-IR spectroscopy, observing the vanishing azide peak at

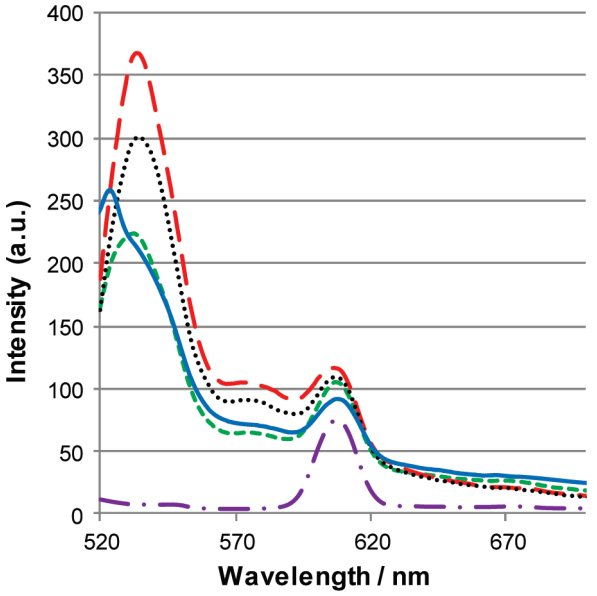


**Figure 1.** Fluorescence spectra of BODIPY-tagged nanoparticles **5** (green broken line), **7** (blue solid line), **12** (red broken line), **13** (black dotted line), and water (purple broken line) as a reference. All spectra were recorded in water at particle concentrations of 0.03 mg/mL. The peak at 608 nm corresponds to the Raman scattering peak of water.[32]

2100 $cm^{-1}$ (Figure 2A). The loading of the particles with BODIPY dye **2** was assessed via elemental microanalysis to be 0.1 mmol/g. Furthermore, a control experiment was performed repeating the reaction without the addition of CuI. The IR spectrum subsequently obtained was equivalent to the spectrum of azide-tagged beads **4**, including the azide peak at 2100 $cm^{-1}$ (spectrum not shown). The absence of peaks corresponding to the BODIPY dye **2** indicated that unspecifically adsorbed molecules were efficiently removed during the washing process.

Fluorescence spectroscopy of particle dispersions in water at a relevant concentration for biological applications (0.03 mg/mL) resulted in a strong emission maximum at 533 nm for noncovalently BODIPY-labeled particles **5** and 524 nm, respectively, for covalently BODIPY-labeled particles **7** (Figure 1). The 505 nm wavelength was chosen as excitation wavelength to avoid detection of scattered light.

Although massive quenching of various fluorescent dyes on carbon surfaces is reported in the literature,[20−22] our measurements clearly show a strong remaining fluorescence of the BODIPY dyes after covalent as well as noncovalent immobilization (Figure 2). In the case of the noncovalently attached fluorescent label, pyrene is considered to bind more effectively to the graphene surface through its extended $\pi$-system, thus hampering quenching effects by keeping the BODIPY dye away from the surface.

The possible quenching could not be quantified for aqueous systems because it was not possible to dissolve relevant amounts of pyrene-tagged BODIPY **3** in water to prepare reference solutions. Organic solvents are not compatible with noncovalently functionalized nanoparticles because they remove considerable amounts of dye from the carbon surface. For the covalently functionalized particles **7**, however, quenching effects were examined in toluene. In a nanoparticle dispersion comprising a $10^{-9}$ M concentration of immobilized dye (calculated by

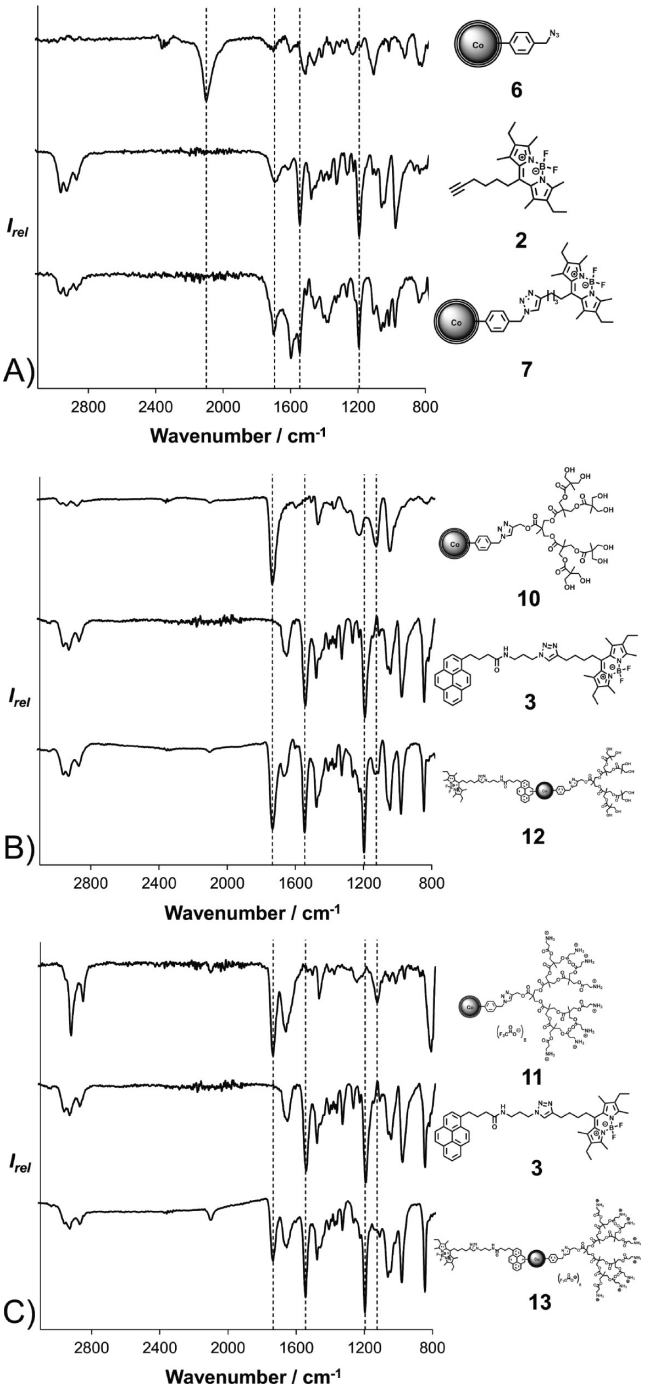


**Figure 2.** IR Spectra depicting the transformation of azide-functionalized nanoparticles **6** to BODIPY-tagged particles **7** (A) and the noncovalent functionalization of dendrimer-loaded nanoparticles **10** (B) and **11** (C) with BODIPY dye. Successful covalent functionalization can be monitored by the vanishing azide peak at 2100 $cm^{-1}$.

elemental analysis), only 36% of the fluorescence intensity was quenched in respect to a reference solution with the same concentration.[28]

To further evaluate fluorescence labeling and to monitor the distribution of the fluorescent dye across the nanoparticles, confocal laser scanning microscopy (CLSM)[29] was used. The confocal arrangement of light source (argon laser, 514 nm excitation wavelength) and detector allows only light emitted


dx.doi.org/10.1021/cm200705d |*Chem. Mater.* 2011, 23, 3606–3613

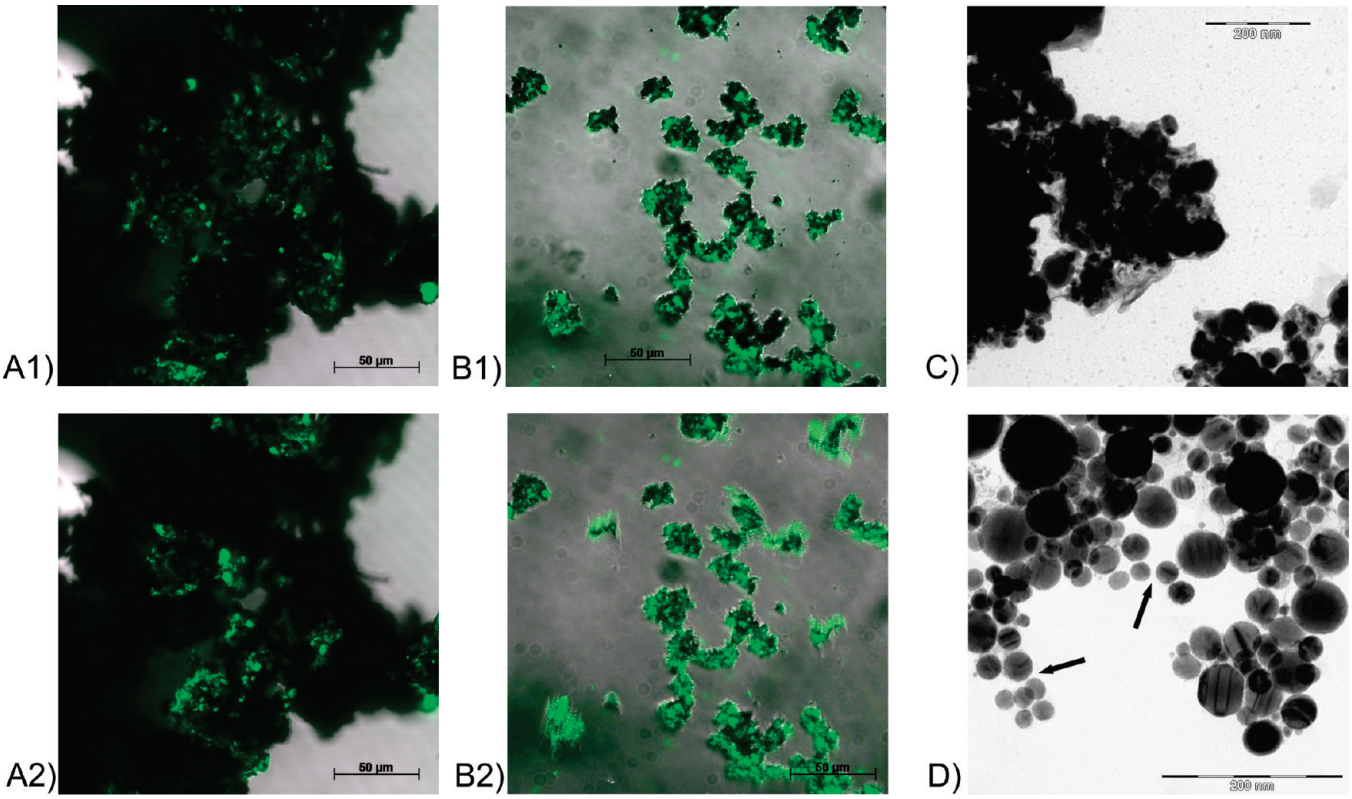


**Figure 3.** CLSM pictures of noncovalently BODIPY-labeled Co/C nanoparticles **5** [A1 and A2 (two different focal planes)] and covalently labeled particles **7** [B1 (one focal plane) and B2 (overlay of 15 pictures taken in different focal planes)]. Black spots correspond to Co/C nanoparticles in shining-through light, while green spots are related to immobilized BODIPY fluorescent dye. TEM image of pristine nanoparticles **4** (C) and dendrimer coated nanobeads **10** (D). Bar lengths are 50 $\mu$m for CLSM and 200 nm for TEM, respectively.[28,32]

from the focal plane to be focused at the detector and therefore measured. By this means, different focal planes can be observed, and a z-stack of pictures is created, providing three-dimensional information of the fluorescent labeling. Z-stacks of noncovalently BODIPY-labeled Co/C nanoparticles **5** (Figure 3A) and covalently labeled nanobeads **7** (Figure 3B) were recorded by CLSM. In these pictures, the intense fluorescence of the immobilized BODIPY dye is clearly visible in the focal planes, and it appears that the labeling is quite evenly spread across the particle agglomerates. The resolution of the CLSM is not high enough to depict single nanoparticles (scale bar = 50 $\mu$m), and thus, although complete surface coverage is likely as judged by sampling through different focal planes (Figure 3 and Supporting Information), it cannot be visualized on the nanoscale by this method. Sections showing reduced or no fluorescence could arise from agglomeration of the nanoparticles during the functionalization process but more likely from nanoparticles outside of the focal planes excited in these pictures. Overlaying multiple pictures (Figure 3B2) clearly shows high, if not uniform, fluorescent labeling of the nanoparticles. Parts with increased fluorescence could originate from a higher aggregation of nanoparticles in this area combined with the excitation of a multitude of nanoparticles on the *z*-axis.

Although pictures taken by CSLM only represent a very small part of the sample, it seems that the covalently functionalized particles are better separated. The irreversible functionalization via diazonium ions might hamper the agglomeration of the nanoparticles to some extent, while the noncovalent functionalization with pyrene-tagged BODIPY is apparently not sufficient to prevent considerable agglomeration of the nanoparticles. The higher aggregation of noncovalently functionalized nanobeads **5** might also explain its reduced loading with dye molecules as determined by elemental microanalysis.

As the next step, the dual functionalization of the graphene-like surface was investigated. The nanoparticles were covalently functionalized with polyester dendrons based on 2,2-bis-(hydroxymethyl) propionic acid (Scheme 3).[16] These dendrons are comercially available, biocompatible, and feature a high multiplicity of surface sites. Dendrons with alkyne groups at the focal point and either hydroxy (**8**)[30] or ammonium groups (**9**)[31] at the periphery were synthesized according to literature procedures and then covalently grafted on azide-tagged nanoparticles **6** through a CuAAC[27] reaction. $CuSO_4 \cdot 5H_2O$ and sodium ascorbate in a THF/water mixture were applied taking into account the high polarity of the dendrons.

By this method, functionalization of the nanoparticles with a loading of 0.04 mmol/g (0.32 mmol FG/g) in the hydroxyl and 0.02 mmol/g (0.16 mmol FG/g) in the ammonium terminated dendrimer (**10** and **11**) could be realized as estimated by elemental microanalysis. The control experiment in the absence of $CuSO_4$ revealed that after the usual washing procedure no dendrimers on the nanoparticle surface could be detected by ATR-IR (spectrum not shown). Additionally, an image recorded by transmission electron microscopy (TEM) of dendrimer-functionalized nanobeads **10** was obtained (Figure 3D). Although the dendrimers cannot be visualized by this method, improved separation of the single nanoparticles is apparent (arrows) compared to the TEM of unmodified nanoparticles **4** (Figure 3C).

**Scheme 3. Combined Covalent and Noncovalent Functionalization of Co/C Nanoparticles. (TFA = Trifluoroacetic Acid)**

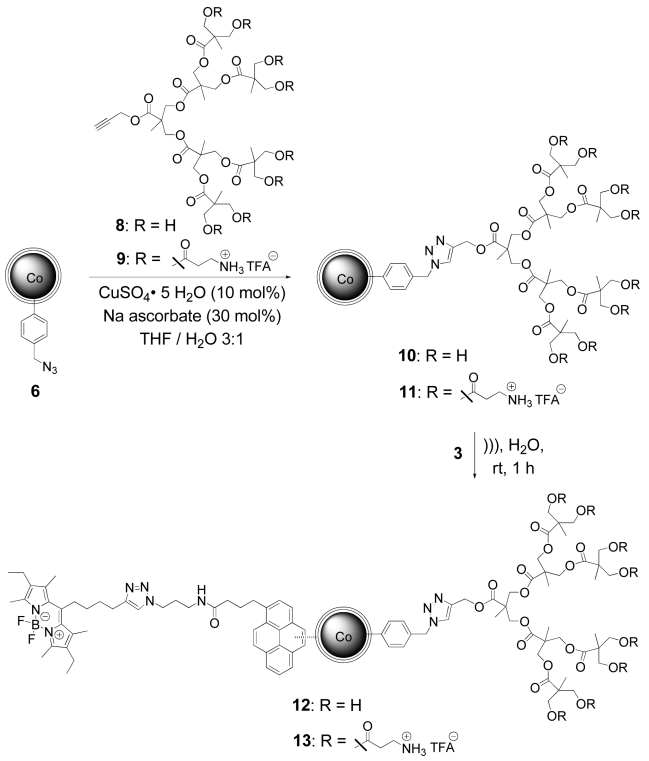


Subsequently, a noncovalent functionalization with BODIPY dye was carried out with **10** and **11**. This dual functionalization strategy was chosen over the reversed approach (covalent attachment of dye and noncovalent functionalization with dendrimers) because the second functionalization step could be easily monitored by fluorescence spectroscopy and CLSM. Furthermore, the consecutive covalent and noncovalent approach might be advantageous over randomly "clicking" two alkyne-modified molecules because every functionalization step can be quantified by elemental analysis, and moreover, the noncovalent functionalization can be reversed if desired. To achieve the additional noncovalent functionalization the dendrimer-coated particles, **10** and **11** were sonicated with pyrene-tagged BODIPY dye **3** in water, followed by repetitive washing with water. The immobilization was monitored by ATR-IR (Figure 2B,C). The IR-spectra recorded for multifunctionalized particles **12** and **13** exhibit the characteristic peaks for ester-based dendrimers as well as for the BODIPY dye.

Elemental microanalysis revealed 0.18 mmol/g loading with BODIPY dye for nanoparticles **12** and 0.15 mmol/g for **13**, respectively. The loadings achieved correspond to about 0.5−1 dye molecules per functional group on the dendrimer. They are considerably higher than loadings of nanoparticles **5**, which lack the dendrimers. As stated above, a possible explanation for this result could be the high aggregation and limited dispersibility of the pristine nanobeads **4** in water due to the high magnetism and hydrophobic surface. This aggregation could block the surface for functionalization. Dendrimer-coated nanoparticles (**10** and **11**), on the other hand, exhibit considerably higher dispersion stabilities in water when compared to pristine nanobeads **4**.[28] This might arise from the breakdown of aggregates during the covalent functionalization pathway as well as the polar nature of the dendrimers. However, dispersion stabilities of some months, as observed for dendrimer-coated SWNTs,[26] are difficult to obtain with these highly ferromagnetic nanoparticles because considerable remanent magnetization leads to agglomeration of the beads. The high magnetism, though, enables the easy recovery from reaction mixtures and is beneficial in applications like MRI and hyperthermia.[12,13]

To evaluate, if interactions of the pyrene-BODIPY **3** with the immobilized dendrimers can be considered as a factor for these high loadings, a test reaction was performed. Pyrene-tagged dye **3** was sonicated with an equal amount of *water-soluble* hydroxyl terminated dendrimer **8** in water following the procedure for the noncovalent attachment of **3** onto dendrimer-coated nanoparticles. After the removal of undissolved dye through filtration, a defined volume of the solution was subjected to freeze-drying, and afterward the residue was redissolved in toluene. This detour was necessary because it was not possible to prepare a reference solution of **3** in water as stated above; however, **3** is readily soluble in *toluene*. A control experiment was performed following this procedure but leaving out the addition of dendrimer. By fluorescence spectroscopy, it was determined that only 0.70 $\mu$M of pyrene-BODIPY **3** is soluble in water. The solution without dendrimers was further used as a blank for the measurement of the amount of **3** bound to the dendrimers. By comparison with reference solutions of **3** in toluene, the additional amount of dye kept in solution by interaction with dendrimers was determined as 0.16% of the introduced dye.[28] This is equal to around 600 molecules of dendrimer per dye molecule, while on the nanoparticles the relation between dendrimer branches and dye molecules is 1:4.5 in favor of dye molecules. This experiment showed that there is an interaction between pyrene-tagged BODIPY and hydroxyl-terminated dendrimers, although the amount of dye bound to dendrimers is negligible, which is no surprise regarding the unpolar nature of the pyrene moiety and the rather polar nature of the dendrimers. The same should be true for dendrimers covalently bound to the nanoparticles leading to the conclusion that the vast majority of immobilized dye **3** in multifunctionalized nanoparticles **12** and **13** is bound to the surface of the nanoparticles rather than to the surface of the dendrimers.

The multifunctionalized particles **12** and **13** emit with 534 nm in the same range as noncovalently BODIPY-labeled nanoparticles **5** (533 nm) when excited at 505 nm in water (Figure 1). At the same particle concentration, however, the intensity of the fluorescence signal is considerably higher for the dendrimer-modified particles corresponding to the higher loading with BODIPY dye. Again, CLSM produced z-stacks of pictures (Figure 4 and Supporting Information), proving that the area-wide functionalization with BODIPY dye was successful even with previous covalent functionalization of the nanoparticle surface.

To examine, if the noncovalent binding of **3** onto the nanoparticle surface is reversible, even if dendrimer branches are present on the surface, multifunctionalized nanoparticles **13** were stirred in toluene for 2 h. The solution was decanted, and the concentration of free dye **3** was determined by fluorescence spectroscopy. This procedure was repeated twice. The amount of released dye was then compared with the amount of immobilized dye measured by elemental microanalysis (0.15 mmol/g). In the first washing step, 95.3% (0.143 mmol/g) of the immobilized dye was released into solution followed by 3.3% (0.005 mmol/g) in

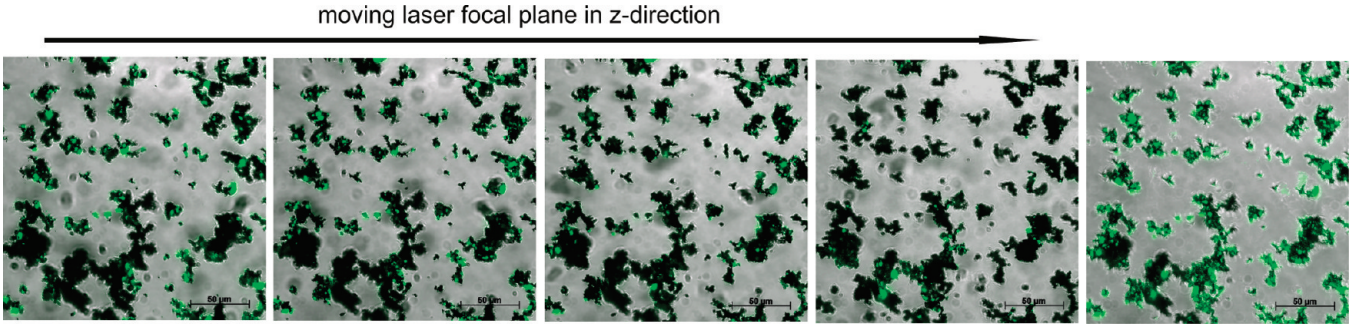


**Figure 4.** Z-stack of four CLSM pictures (bar length 50 $\mu$m) showing noncovalently BODIPY and covalently [G3]-$(NH_3^+TFA^-)_8$ functionalized Co/C nanoparticles **13**, excitation wavelength 514 nm. The final picture shows an overlay of 10 CLSM pictures taken in different focal planes.[32]

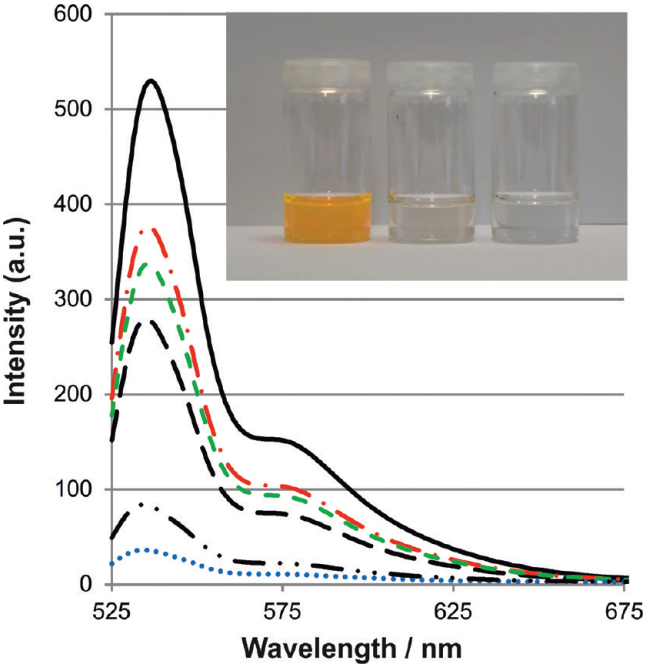


**Figure 5.** Washing solution 1 (diluted 1:25, red broken line), 2 (green broken line), and 3 (blue dotted line) of multifunctionalized nanobeads **13** in toluene and the corresponding reference solutions of dye **3** at concentrations of 4.32 $\mu$M (black solid line), 2.16 $\mu$M (black broken line), and 0.86 $\mu$M (black broken and dotted line). The inserted picture is showing washing solution 1, 2, and 3 (from left to right).[32]

the second step (Figure 5). In the third step, however, less than 0.1% of the total amount of bound dye was released from the particle surface. Altogether, this experiment showed that the noncovalent functionalization of carbon-coated nanobeads with pyrene-tagged dye can be reversed by more than 98% in only two washing cycles regardless of the additional covalent functionalization with dendrimers.

## CONCLUSIONS

In summary, we have demonstrated that it is possible to covalently as well as noncovalently functionalize graphene surfaces with functional molecules such as BODIPY. By fluorescence spectroscopy and CLSM, we have proven that both functionalization pathways render the particles highly fluorescent, which is a key feature for the application of these nanoparticles in the field of bioimaging. In further experiments, we have also shown that it is possible to noncovalently bind a dye to the nanoparticles with a prevalent covalent coating. This system represents a new approach toward multifunctional carbon nanomaterials and should be a promising starting point for a broad range of biomedical applications, making use of the possibility to attach drugs or targeting molecules at the periphery of the dendrimers and simultaneously label the particles noncovalently with the BODIPY dye. Furthermore, relying only on MRI for imaging the dye could also be exchanged for a drug, allowing multifunctionalization of the particles with drug and targeting molecules. Such investigations are ongoing in our laboratories.

## ASSOCIATED CONTENT

**Supporting Information.** Detailed characterization data for the organic compounds and additional UV/vis, fluorescence and IR spectras as well as CLSM pictures. This material is available free of charge via Internet at http://pubs.acs.org.

## AUTHOR INFORMATION

**Corresponding Author**
*E-mail: Oliver.Reiser@chemie.uni-regensburg.de.

## ACKNOWLEDGMENT

This work is supported by the Deutsche Forschungsgemeinschaft (Re 948/8-1, "GLOBUCAT") and the IDK NANOCAT (Elitenetzwerk Bayern). Turbobeads Llc, Switzerland, is acknowledged for a generous donation of nanoparticles.

## REFERENCES

(1) (a) Maggini, M.; Scorrano, G.; Prato, M. *J. Am. Chem. Soc.* **1993**, *115*, 9798–9799. (b) Hirsch, A.; Lamparth, I.; Karfunkel, H. R. *Angew. Chem., Int. Ed.* **1994**, *33*, 437–438. (c) Kräutler, B.; Maynollo, J. *Angew. Chem., Int. Ed.* **1995**, *34*, 87–88. (d) Diederich, F.; Thilgen, C. *Science* **1996**, *271*, 317–323. (e) Prato, M. *J. Mater. Chem.* **1997**, *7*, 1097–1109. (f) Diederich, F.; Gómez-López, M. *Chem. Soc. Rev.* **1999**, *28*, 263–277.

(2) (a) Holzinger, M.; Vostrowsky, O.; Hirsch, A.; Hennrich, F.; Kappes, M.; Weiss, R.; Jellen, F. *Angew. Chem., Int. Ed.* **2001**, *40*, 4002–4005. (b) Niyogi, S.; Hamon, M. A.; Hu, H.; Zhao, B.; Bhowmik, P.; Sen, R.; Itkis, M. E.; Haddon, R. C. *Acc. Chem. Res.* **2002**, *35*, 1105–1113. (c) Singh, P.; Campidelli, S.; Giordani, S.; Bonifazi, D.; Bianco, A.; Prato, M. *Chem. Soc. Rev.* **2009**, *38*, 2214–2230. (d) Karousis, N.; Tagmatarchis, N. *Chem. Rev.* **2010**, *110*, 5366–5397. (e) Bose, S.; Khare, R. A.; Moldenaers, P. *Polymer* **2010**, *51*, 975–993.

(3) (a) Grass, R. N.; Athanassiou, E. K.; Stark, W. J. *Angew. Chem.* **2007**, *119*, 4996–4999. (b) Tan, C. G.; Grass, R. N. *Chem. Commun.*

**2008**, 4297–4299. (c) Schätz, A.; Grass, R. N.; Stark, W. J.; Reiser, O. *Chem.—Eur. J.* **2008**, *14*, 8262–8266. (d) Fuhrer, R.; Athanassiou, E. K.; Luechinger, N. A.; Stark, W. J. *Small* **2009**, *5*, 383–388. (e) Herrmann, I. K.; Grass, R. N.; Mazunin, D.; Stark, W. J. *Chem. Mater.* **2009**, *21*, 3275–3281. (f) Schätz, A.; Grass, R. N.; Kainz, Q.; Stark, W. J.; Reiser, O. *Chem. Mater.* **2010**, *22*, 305–310. (g) Schätz, A.; Long, T. R.; Grass, R. N.; Stark, W. J.; Hanson, P. R.; Reiser, O. *Adv. Funct. Mater.* **2010**, *20*, 4323–4328. (h) Maity, P. K.; Rolfe, A.; Samarakoon, T. B.; Faisal, S.; Kurtz, R. D.; Long, T. R.; Schätz, A.; Flynn, D. L.; Grass, R. N.; Stark, W. J.; Reiser, O.; Hanson, P. R. *Org. Lett.* **2011**, *13*, 8–11. (i) Schätz, A.; Stark, W. J.; Reiser, O. *Chem.—Eur. J.* **2010**, *16*, 8950–8967. (j) Shylesh, S.; Schünemann, V.; Thiel, W. R. *Angew. Chem., Int. Ed. Engl.* **2010**, *49*, 3428–3459.

(4) Bianco, A.; Pastorin, G.; Wu, W.; Wieckowski, S.; Briand, J.-P.; Kostarelos, K.; Prato, M. *Chem. Commun.* **2006**, 1182–1184.

(5) Shi, X.; Wang, S. H.; Shen, M.; Antwerp, M. E.; Chen, X.; Li, C.; Petersen, E. J.; Huang, Q.; Weber, W. J.; Baker, J. R. *Biomacromolecules* **2009**, *10*, 1744–1750.

(6) (a) Lee, K. M.; Li, L.; Dai, L. *J. Am. Chem. Soc.* **2005**, *127*, 4122–4123. (b) Wu, W.; Wieckowski, S.; Pastorin, G.; Benincasa, M.; Klumpp, C.; Briand, J.-P.; Gennaro, R.; Prato, M.; Bianco, A. *Angew. Chem., Int. Ed.* **2005**, *44*, 6358–6362. (c) Stephenson, J. J.; Hudson, J. L.; Leonard, A. D.; Price, B. K.; Tour, J. M. *Chem. Mater.* **2007**, *19*, 3491–3498. (d) Brunetti, F. G.; Herrero, M. A.; Munõz, J. de M.; Díaz-Ortiz, A.; Alfonsi, J.; Meneghetti, M.; Prato, M.; Vázquez, E. *J. Am. Chem. Soc.* **2008**, *130*, 8094–8100. (e) Rubio, N.; Herrero, M. A.; de la Hoz, A.; Meneghetti, M.; Prato, M.; Vázquez, E. *Org. Biomol. Chem.* **2010**, *8*, 1936–1942.

(7) (a) Chen, R. J.; Zhang, Y.; Wang, D.; Dai, H. *J. Am. Chem. Soc.* **2001**, *123*, 3838–3839. (b) Georgakilas, V.; Kordatos, K.; Prato, M.; Guldi, D. M.; Holzinger, M.; Hirsch, A. *J. Am. Chem. Soc.* **2001**, *124*, 760–761. (c) Gómez, F. J.; Chen, R. J.; Wang, D.; Waymouth, R. M.; Dai, H. *Chem. Commun.* **2003**, 190–191. (d) Liu, G. L.; Wu, B.; Zhang, J.; Wang, X.; Shao, M.; Wang, J. *Inorg. Chem.* **2009**, *48*, 2383–2390. (e) Nakashima, N.; Tomonari, Y.; Murakami, H. *Chem. Lett.* **2002**, 638–639. (f) McQueen, E. W.; Goldsmith, J. I. *J. Am. Chem. Soc.* **2009**, *131*, 17554–17556.

(8) Wittmann, S.; Schätz, A.; Grass, R. N.; Stark, W. J.; Reiser, O. *Angew. Chem., Int. Ed.* **2010**, *49*, 1867–1870.

(9) Müller, C.; Hampel, S.; Elefant, D.; Biedermann, K.; Leonhardt, A.; Ritschel, M.; Büchner, B. *Carbon* **2006**, *44*, 1746–1753.

(10) (a) Lu, A.-H.; Li, W.; Matoussevitch, N.; Spliethoff, B.; Bönnemann, H.; Schüth, F. *Chem. Commun.* **2005**, 98–100. (b) Seo, W. S.; Lee, J. H.; Sun, X. M.; Suzuki, Y.; Mann, D.; Liu, Z.; Terashima, M.; Yang, P. C.; Mc Connell, M. V.; Nishimura, D. G.; Dai, H. J. *Nature Mat.* **2006**, *5*, 971–976. (c) Liang, Y.-C.; Huang, K. C.; Lo, S.-C. *Small* **2008**, *4*, 405–409.

(11) (a) Widder, K. J.; Senyei, A. E.; Scarpelli, D. G. *Proc. Soc. Exp. Biol. Med.* **1978**, *58*, 141–146. (b) Douziech-Eyrolles, L.; Marchais, H.; Hervé, K.; Munnier, E.; Soucé, M.; Linassier, C.; Dubois, P.; Chourpa, I. *Int. J. Nanomed.* **2007**, *2*, 541–550.

(12) (a) Pankhurst, Q. A.; Connolly, J.; Jones, S. K.; Dobson, J. *J. Phys. D* **2003**, *36*, R167–R181. (b) Mornet, S.; Vasseur, S.; Grasset, F.; Duguet, E. *J. Mater. Chem.* **2004**, *14*, 2161–2175. (c) Corot, C.; Robert, P.; Idee, J. M.; Port, M. *Adv. Drug Delivery Rev.* **2006**, *58*, 1471–1504.

(13) (a) Ito, A.; Shinkai, M.; Honda, H.; Kobayashi, T. *J. Biosci. Bioeng.* **2005**, *100*, 1–11. (b) Ivkov, R.; DeNardo, S. J.; Daum, W.; Foreman, A. R.; Goldstein, R. C.; Nemkov, V. S.; DeNardo, G. L. *Clin. Cancer. Res.* **2005**, *11*, 7087s–7092s.

(14) Mikhaylova, M.; Kim, D. K.; Bobrysheva, N.; Osmolowsky, M.; Semenov, V.; Tsakalakos, T.; Muhammed, M. *Langmuir* **2004**, *20*, 2472–2477.

(15) (a) Koehler, F. M.; Rossier, M.; Waelle, M.; Athanassiou, E. K.; Limbach, L. K.; Grass, R. N.; Günther, D.; Stark, W. J. *Chem. Commun.* **2009**, 4862–4864. (b) Rossier, M.; Koehler, F. M.; Athanassiou, E. K.; Grass, R. N.; Aeschlimann, B.; Günther, D.; Stark, W. J. *J. Mater. Chem.* **2009**, *19*, 8239–8243.

(16) (a) Ihre, H.; Hult, A. *J. Am. Chem. Soc.* **1996**, *118*, 6388. (b) Ihre, H.; Hult, A.; Fréchet, J. M. J.; Gitsov, I. *Macromolecules* **1998**, *31*, 4061. (c) Malkoch, M.; Malström, E.; Hult, A. *Macromolecules* **2002**, *35*, 8307.

(17) Xu, C.; Sun, S. *Dalton Trans.* **2009**, 5583–5591.

(18) (a) De Jesús, O. L. P.; Ihre, H. R.; Gagne, L.; Fréchet, J. M. J.; Szoka, F. C. *Bioconjugate Chem.* **2002**, *13*, 453–461. (b) Medina, S. H.; El-Sayed, M. E. H. *Chem. Rev.* **2009**, *109*, 3141–3157.

(19) Lee, H.; Yu, M. K.; Park, S.; Moon, S.; Min, J. J.; Jeong, Y. Y.; Kang, H. W.; Jon, S. *J. Am. Chem. Soc.* **2007**, *129*, 12739–12745.

(20) (a) Fu, C.; Meng, L.; Lu, Q.; Fei, Z.; Dyson, P. J. *Adv. Funct. Mater.* **2008**, *18*, 857–864. (b) Zhang, X; Meng, L; Wang, X; Lu, Q. *Chem.—Eur. J.* **2009**, *16*, 556–561. (c) Nakayama-Ratchford, N.; Bangsaruntip, S.; Sun, X.; Welsher, K.; Dai, H. *J. Am. Chem. Soc.* **2007**, *129*, 2448–2449. (d) Yang, R.; Jin, J.; Chen, Y.; Shao, N.; Kang, H.; Xiao, Z.; Tang, Z.; Wu, Y.; Zhu, Z.; Tan, W. *J. Am. Chem. Soc.* **2008**, *130*, 8351–8358. (e) Ahmad, A.; Kurkina, T.; Kern, K.; Balasubramanian, K. *Chem. Phys. Chem.* **2009**, *10*, 2251–2255.

(21) (a) Swathiand, R. S.; Sebastian, K. L. *J. Chem. Phys.* **2008**, *129*, 054703/1–9. (b) Cho, E. S.; Hong, S. W.; Jo, W. H. *Macromol. Rapid Commun.* **2008**, *29*, 1798–1803. (c) Tasis, D.; Mikroyannidis, J.; Karoutsos, V.; Galiotis, C.; Papagelis, K. *Nanotechnology* **2009**, *20*, 135606–135613.

(22) (a) Yang, R.; Tang, Z.; Yan, J.; Kang, H.; Kim, Y.; Zhu, Z.; Tan, W. *Anal. Chem.* **2008**, *80*, 7408–7413. (b) Zhao, C.; Qu, K.; Song, Y.; Xu, C.; Ren, J.; Qu, X. *Chem.—Eur. J.* **2010**, *16*, 8147–8154. (c) Zhang, L.; Li, T.; Li, B.; Li, J.; Wang, E. *Chem. Commun.* **2010**, *46*, 1476–1478. (d) Chang, H.; Tang, L.; Wang, Y.; Jiang, J.; Li, J. *Anal. Chem.* **2010**, *82*, 2341–2346.

(23) (a) Treibs, A.; Kreuzer, F.-H. *Liebigs Ann. Chem.* **1968**, *718*, 208–223. (b) Vos de Wael, E.; Pardoen, J. A.; van Koeveringe, J. A.; Lugtenburg, J. *Recl. Trav. Chim. Pays-Bas* **1977**, *96*, 306–309. (c) Karolin, J.; Johansson, L. B.-A; Strandberg, L.; Ny, T. *J. Am. Chem. Soc.* **1994**, *116*, 7801–7806.

(24) Verdoes, M.; Hillaert, U.; Florea, B. I.; Sae-Heng, M.; Risseeuw, M. D. P.; Filippov, D. V.; van der Marel, G. A.; Overkleeft, H. S. *Bioorg. Med. Chem. Lett.* **2007**, *17*, 6169–6171.

(25) Rossier, M.; Koehler, F. M.; Athanassiou, E. K.; Grass, R. N.; Aeschlimann, B.; Günther, D.; Stark, W. J. *J. Mater. Chem.* **2009**, *19*, 8239–8243.

(26) Wu, P.; Chen, X.; Hu, N.; Tam, U. C.; Blixt, O.; Zettl, A.; Bertozzi, C. R. *Angew. Chem., Int. Ed.* **2008**, *47*, 5022.

(27) (a) Tornøe, C. W.; Meldal, M. In *Peptidotriazoles: Copper(I)-Catalyzed 1,3-Dipolar Cycloadditions on Solid-Phase*; Lebl, M., Houghten, R. A., Eds.; American Peptide Society and Kluwer Academic Publishers: San Diego, 2001; pp 263−264. (b) Rostovsev, V. V.; Green, L. G.; Fokin, V. V.; Sharpless, K. B. *Angew. Chem., Int. Ed.* **2002**, *41*, 2596–2599. (c) Tornøe, C. W.; Christensen, C.; Meldal, M. *J. Org. Chem.* **2002**, *67*, 3057–3064. (d) Lolber, S.; Rodriguez-Loaiza, P.; Gmeiner, P. *Org. Lett.* **2003**, *5*, 1753.

(28) See Supporting Information.

(29) (a) Wijnaendts Van Resandt, R. W.; Marsman, H. J. B.; Kaplan, R.; Davoust, J.; Stelzer, E. H. K.; Stocker, R. *J. Microsc.* **1985**, *138*, 29–34. (b) Van der Voort, H. T. M.; Brakenhoff, G. J.; Valkenburg, J. A. C.; Nanninga, N. *Scanning* **1985**, *7*, 66–78. (c) Minsky, M. *Scanning* **1988**, *10*, 128–138.

(30) Wu, P.; Malkoch, M.; Hunt, J. N.; Vestberg, R.; Kaltgrad, E.; Finn, M. G.; Fokin, V. V.; Sharpless, K. B.; Hawker, C. J. *Chem. Commun.* **2005**, 5775–5777.

(31) Li, B.; Martina, A. L.; Gillies, E. R. *Chem. Commun.* **2007**, 5217–5219.

(32) Colored pictures can be found within the online version.